287. The Transient behavior of rails used in electromagnetic railguns: numerical investigations at constant loading velocities

L. Tumonis[1, a], R. Kačianauskas[1,b], A. Kačeniauskas[2,c], M. Schneider[3,d]
[1]Department of Strength of Materials, Vilnius Gediminas Technical University, Saulėtekio 11, 10223 Vilnius, Lithuania
[2]Laboratory of Parallel Computing, Vilnius Gediminas Technical University, Saulėtekio 11, 10223 Vilnius, Lithuania
[3] French-German Research Institute of Saint Louis (ISL), 5 rue G'al Cassagnou, 68301 Saint-Louis, France
E-mail: [a]*liudas.tumonis@fm.vgtu.lt,* [b]*rkac@fm.vgtu.lt,* [c]*arnka@fm.vgtu.lt,* [d]*schneider_m@isl.tm.fr*

Abstract. Electromagnetic railguns are mechatronic systems working at very high power levels (in the range of GW). Here, one important issue, namely, the dynamical reaction of the rails and their supporting structure to the moving (due to the projectile) magnetic pressure loads is still not sufficiently described.

In this paper the above described problem is investigated using a purely mechanical 2D finite element model. The aim is to describe the displacement of the rail surfaces because of its importance for the electrical performance of the system. The boundary conditions correspond to the moving electromagnetic pressure repelling the rails one from each other. The oscillation profiles under several loading histories with constant velocities ranging between 0.6 and 1.4 km/s are examined.

Keywords: Electromagnetic railgun, transient dynamics.

Introduction

Electromagnetic railguns are mechatronic systems working at very high power levels (in the range of GW). While the functional principle is relatively simple and muzzle velocities up to 2.5 km/s for masses of several hundred grams have been demonstrated experimentally the performance limits of the technique are still under investigation worldwide [1-3]. Here, due to its influence on electric contact conditions, one important point is the dynamical reaction of the rails and their supporting structure to the moving (due to the projectile) magnetic pressure [4, 5].

The functional principle of the railgun is illustrated in Fig. 1. The projectile has a conducting part (armature). This armature is in sliding contact with two rails which are connected to a power source being able to deliver the current in the order of MA. The magnetic pressure (in the order of 100 MPa) generated by this configuration not only propels the projectile via the armature but also repels the rails one from the other. One of the most critical parts of the system is the contact interface between armatures and rails where enormous current densities (up to kA/mm^2) have to exist while simultaneously low friction forces have to be established. The dynamical interaction at this contact interface presents a great challenge to all scientists working in this interdisciplinary research area. The railgun EMA3 of the French German Research institute of Saint-Louis (ISL) is depicted in Fig. 2 [6]. EMA3 has rails with a length of 3 m and a caliber of 15x30 mm^2. The housing of the rails is not closed laterally which permits flash radiography during launch. Projectiles with masses of 50 g have been accelerated to velocities of up to 1800 m/s with excellent sliding contact behavior [7].

In this paper the mechanical behavior of EMA3 is simulated numerically. The aim is to study an important aspect of the contact interface, namely the displacement of the inner rail surfaces due to the magnetic pressure mentioned above.

Finite element calculations concerning the mechanical behavior of EMA3 have been performed with ANSYS[1] [8]. In order to simplify the problem the railgun is represented by an axisymmetric 2D model of the rails and discrete elastic supports. The boundary conditions of loading correspond to the magnetic pressure that expands with very high velocities behind the projectile. It is interesting to mention that the velocity of the projectile can be in the range and even greater than those of elastic waves in the rails.

At this stage a constant velocity of the movement of the magnetic pressure is assumed. Results are presented for different loading velocities (0.6 km/s-1.4 km/s).

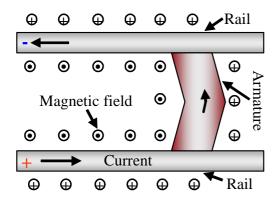[1] ANSYS is a trademark of Ansys Inc.

Fig. 1. Functional principle of the rail gun

Fig. 2. The ISL-railgun EMA3

Problem description. Rail geometry, material data and loading

A view of the railgun cross-section is shown in Fig. 3. The housing of the two rails consists of a combination of bars of EPM 203, a glass fiber reinforced plastics (GRP) material, and discontinuous steel bolts in order to withstand the high forces between the rails. At both sides of the rails GRP-bars are used to guide the projectile.

The rails are made from a Cu alloy (CRM 16N). The material properties used for the numerical calculations of the railgun are given in Table 1.

In this paper in a first step the boundary conditions for the calculations (loading) are simplified by comparison to the

experiment. Only the expansion of the magnetic pressure volume being caused by the moving projectile is considered and not local transversal forces due to the projectile itself. It is assumed that the expansion takes place at a constant velocity and that the magnetic pressure is not time-dependent but has a constant value $q = 31.2$ MPa. This value corresponds to experiments presented in [6].
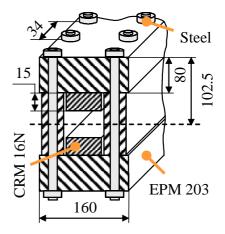

Fig. 3. Cross-section of the railgun

Therefore, the load profile at an arbitrary point x along the direction of movement is defined by the following equation

$$q(x, x_f) = \begin{cases} q, & \text{if } x \leq x_f, \\ 0, & \text{if } x > x_f, \end{cases} \qquad (1)$$

where x_f represents the position of the load front (projectile) at time point t:

$$x_f(t) = vt, \qquad (2)$$

and v is the constant velocity of the projectile.

Table 1. Material properties

Structural member	Material	Physical properties
Housing	EPM 203	Density: $\rho = 1.85$ g/cm^3 Elast. modulus: $E = 18.0$ GPa Poisson's ratio: $\nu = 0.3$
Rail	CuCr1Zr (CRM 16N)	Density: $\rho = 8.90$ g/cm^3 Elast. modulus: $E = 120$ GPa Poisson's ratio: $\nu = 0.3$
Bolt	Steel	Density: $\rho = 7.85$ g/cm^3 Elast. modulus: $E = 210$ GPa Poisson's ratio: $\nu = 0.3$

16

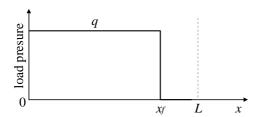The load profile along entire rail length L is illustrated in Fig. 4.
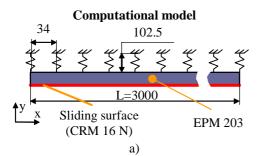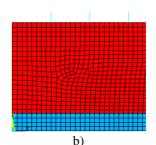

Fig. 4. Load profile

In order to save computational time a 2D model has been developed and due to symmetry reasons only half of the cross section is considered. The rails and the GRP bars are represented by a T-shaped bimaterial profile (see Fig. 3). The steel bolts are transformed into elastic rods. The mechanical characteristics of these rods are equivalent to the bolts.

The rail is considered as 2D domain, while the supporting rods are modeled as elastic springs. The computational model of the rail gun is illustrated in Fig. 5.

Fig. 5. 2D model of the rail gun: a) total view, b) fragment of the mesh

The finite element mesh used consists of 18652 2D plane elements. The supporting bolts are approximated by 86 elastic spring elements. The whole model has 56719 degrees of freedom. The loading is defined as normal pressure acting on the rail surfaces.

The dynamic loading profiles are computed with the pre-processing program MOVLOAD written by using C++. The resulting values of the nodal loads are stored in a macro file in native ANSYS [8] format. The file includes information on all load steps for each time point. Macro files are loaded by the specific pre-processor MOVLOAD. This pre-processor automatically computes all values of the nodal loads and significantly reduces time for data preparation. The STRUCTURAL module of the FE-package ANSYS 10.0 was used.

Numerical results and discussion

The described FE model was used for dynamic analysis of the railgun under loading conditions specified above. Four different velocities were simulated including the static case serving as reference. The latter was realized using a fixed loading along the entire rail length.

The dynamic behavior of the rail is characterized by considering the time-dependent displacements in y-direction (Fig. 5) u_y of the nodes belonging to the sliding contact surface. Displacement profiles of the node being in the middle of the rail ($x = 1.5$ m) are drawn in Fig. 6. Here, small circles indicate the time points when the load front reaches the node. It can be seen that dynamic loading leads to oscillations with the static solution acting as offset. However, with regard to the contact conditions the absolute values are of interest and here it has to be stated that amplitudes due to dynamic loading are two times greater than the static ones.
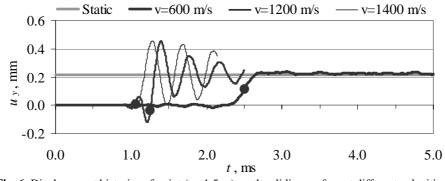

Fig. 6. Displacement histories of point ($x = 1.5$ m) on the sliding surface at different velocities

Note that even variations of some tenth of millimeters are important in this context [6], if they occur at the position of the sliding contact. A comparison of displacement histories of different nodes along the sliding contact surface at a sliding velocity of 1200 m/s is presented in Fig. 7. Here, again circles indicate time points of the load-arrival for the different nodes. The static solution is also presented. Two details should be pointed out here. Firstly, despite the two nodes at 0.75 m and 2.25 m have a symmetric position along the rail with respect to the central node the corresponding displacement profiles are entirely different. Secondly, and of great importance for the railgun: one observes amplitudes of relevant magnitude before the pressure front arrives. These increase in forward direction and are at maximum for the node at 2.25 m.
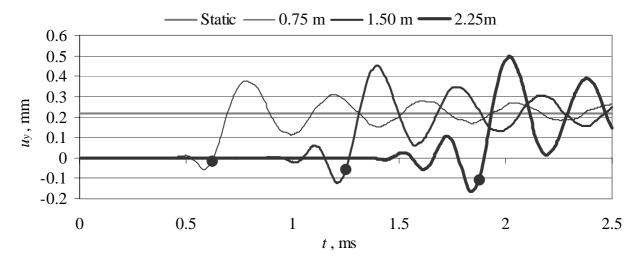

Fig. 7. Displacement histories of different points at velocity v = 1200 m/s

In order to illustrate the dynamic behavior of the rails the concept of the effective amplitude is used. It is illustrated in Fig. 8. The excitation period Δt of a particular node located in position x_n is defined as difference between entire loading period t_{sh} and time interval t_f before the point is loaded. It is expressed in terms of loading data as follows

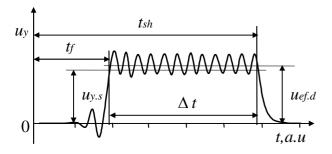$$\Delta t = \frac{(L - x_n)}{v} . \qquad (3)$$

Fig. 8. The concept of effective amplitude

Finally, the effective amplitude $u_{ef.d}$ is obtained using least square method by integrating the difference between dynamic displacements $u_y(t)$ and static solution $u_{y.s}$:

$$u_{ef.d} = \sqrt{\frac{1}{\Delta t} \int_{t_f}^{t_{sh}} \left(u_y(t) - u_{y.s} \right)^2 dt} . \qquad (4)$$

It is obvious that for static behavior $u_{ef.d} = 0$.

The dependence of effective amplitudes (Eq. 4) on the sliding velocity for different locations along the rail is presented in Fig. 9. It shows that the rail dynamics during shot is a rather position-dependent phenomenon. Due to symmetry reasons the behavior of the middle point (1.5 m) of the rail may be considered as the most characteristic of the entire system. If the velocity approaches 1400 m/s a resonance behavior can be stated for this case. Resonance effects are to be expected if the velocity of the projectile reaches the velocity of elastic waves inside the rails [4, 5]. In this context it is interesting to note that for very similar rail geometry to the one considered here the lowest possible velocity for elastic waves inside the rails (Timoshenko beam on elastic foundation) was calculated to be about 1470 m/s [5].
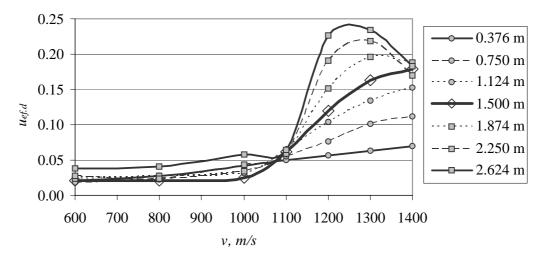
18

Fig. 9. Dependence of effective amplitudes on sliding velocities at different locations

Concluding remarks

A 2D FE model was developed and an effective displacement amplitude method was suggested to investigate the dynamic behavior of the rails with regard to different sliding velocities. The observed resonance velocities differ in the range between 1250 and 1400 m/s depending on the position along the rail. The resonance velocity of the middle point is about 1400 m/s. However, detailed explanation of the resonance phenomenon requires comprehensive future investigations.

References

[1] **Fair H.** IEEE Trans. on Magnetics Vol. 43(1) (2007), p. 93.
[2] **Shvetsov G., Rutberg P. and Budin A.** IEEE Trans. on Magnetics Vol. 43(1) (2007), p. 99.
[3] **Lehmann P., Peter H. and Wey J.** IEEE Trans. on Magnetics Vol. 37 (2001), p. 435.
[4] **Tzeng J. T.** IEEE Trans. on Magnetics Vol. 41(1) 2005, p. 246.
[5] **Johnson A. J. and Moon F. C.** IEEE Trans. on Magnetics Vol. 42(3) (2006), p. 422.
[6] **Schneider M., Eckenfels D. and Hatterer F.** IEEE Trans. on Magnetics Vol. 39 (2003), p. 186.
[7] **Schneider M. and Schneider R.** IEEE Trans. on Magnetics Vol. 41 (2005), p. 432.
[8] ANSYS Theory Reference, 8th edition (SAS IP INC. 2003).